Unsupervised Support Vector Machines for Nonlinear Blind Equalization in CO-OFDM

E. Giacoumidis, A. Tsokanos, M. Ghanbarisabagh, S. Mhatli, and L. P. Barry

Abstract—**A novel blind nonlinear equalization (BNLE) technique based on the iterative re-weighted least square is experimentally demonstrated for single and multi-channel coherent optical orthogonal frequency-division multiplexing (CO-OFDM). The adopted BNLE combines, for the first time, a support vector machine-learning cost function with the classical Sato or Godard error functions and maximum likelihood recursive least-squares. At optimum launched optical power, BNLE reduces the fiber nonlinearity penalty by ~1 (16-QAM single-channel at 2000 km) and ~1.7 dB (QPSK multi-channel at 3200 km) compared to a Volterra-based NLE. The proposed BNLE is more effective for multi-channel configuration: 1) it outperforms the 'gold-standard' digital-back propagation; 2) for a high number of subcarriers the performance is better due to its capability of tackling inter-subcarrier four-wave mixing.**

***Index Terms*—Optical OFDM, Optical Fiber Communication, Machine Learning, Fiber Nonlinearity Compensation.**

I. Introduction

Many electronic techniques have been proposed to compensate fiber nonlinearity such as digital back-propagation (DBP) [1], phase-conjugated twin-waves (PC-TW) [2], maximum-likelihood (ML) with finite impulse response (FIR) filtering [3] and machine learning [4-6, 7]. However, DBP presents enormous computational complexity, PC-TW halves the transmission capacity, while ML-FIR and machine learning require large amount of training data thus limiting the signal capacity. On the other hand, coherent optical OFDM (CO-OFDM) is an excellent candidate for long-haul communications due to its high spectral efficiency and tolerance to both chromatic dispersion (CD) and polarization-mode dispersion (PMD). Yet, due to its high peak-to-average power ratio (PAPR) the nonlinear cross-talk effects among subcarriers are enhanced resulting in complicated nonlinear deterministic noise that appears stochastic. CO-OFDM uses pilot subcarriers to combat linear distortions, while for the compensation of the deterministic fiber nonlinearity it could employ low-complex nonlinear equalization (NLE) based on the inverse Volterra-series transfer function (VNLE) [7]. To tackle stochastic nonlinear noise from the interaction between nonlinearity and random noises (e.g. PMD), CO-OFDM employs nonlinear mapping based on statistical learning such as support vectors machines (SVM) [4-6] and artificial neural networks (ANN) [7] which typically require a large amount of training data. Since blind equalizers are preferred in coherent optical communications as they eliminate inter-symbol interference (ISI) without increasing overhead costs, it is preferably NLEs to compensate linear and nonlinear noises of both deterministic and stochastic nature without the need of training data. To the best of our knowledge, only decision-directed-free blind linear equalizers (LE) [8] have been implemented in CO-OFDM.

This work was emanated from EU Horizon 2020 research and innovation programme under the Marie Skłodowska-Curie grant agreement No 713567 and in part by a research grant from Science Foundation Ireland (SFI) and is co-funded under the European Regional Development Fund under Grant Number 13/RC/2077. We thank Sterlite Techn., S. T. Le (Nokia Bell-labs, Germany), M. E. McCarthy (Oclaro, UK) and A. D. Ellis (Aston University, UK) for their support on this work.

E. Giacoumidis and L. P. Barry are with Dublin City University, Glasnevin 9, Dublin, Ireland (email: {elias.giacoumidis,liam.barry@dcu.ie}).

A. Tsokanos is with University of Hertfordshire, Hatfield, Hertfordshire United Kingdom (a.tsokanos@herts.ac.uk).

M. Ghanbarisabagh is with Department of Electrical Engineering, Faculty of Electrical Engineering and Computer Sciences, Islamic Azad University North Tehran Branch, Tehran, Iran (e-mail: m.ghanbarisabagh@iau-tnb.ac.ir).

S. Mhatli is with Carthage University, SER'Com Laboratory, Tunisia Polytechnic School, Tunisia (sofien_mhatli@yahoo.fr).

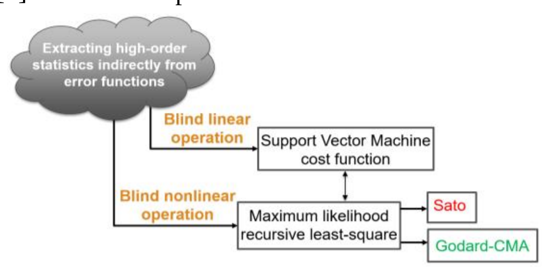

Fig. 1. Conceptual block diagram of proposed blind nonlinear equalizer (BNLE).

In this work, we propose a novel blind NLE (BNLE) based on the iterative re-weighted least square (IRWLS) [9] which combines, for the first time, the conventional cost function of the SVM with the classical Sato or Godard [9] error functions to perform blind LE, and harnesses ML recursive least-squares (ML-RLS) [10,11] for BNLE operation. The proposed hybrid LE/BNLE (referred as BNLE for simplicity throughout this work) is implemented in a single- and multi-channel CO-OFDM setup for ~41-Gb/s 16-quadrature amplitude modulation (16-QAM) at 3200 km and ~21-Gb/s (middle-channel) quaternary phase-shift keying (QPSK) at 2000 km, respectively. It is shown that the developed BNLE can reduce the fiber nonlinearity penalty by ~1.7 and ~1 dB compared to VNLE for multi- and single-channel, respectively, also offering an increase in bit-rate of 1-Gb/s due to the absence of pilot subcarriers. Finally, the proposed BNLE is more effective for high number of subcarriers due to its ability of tackling inter-subcarrier four-wave mixing (FWM).

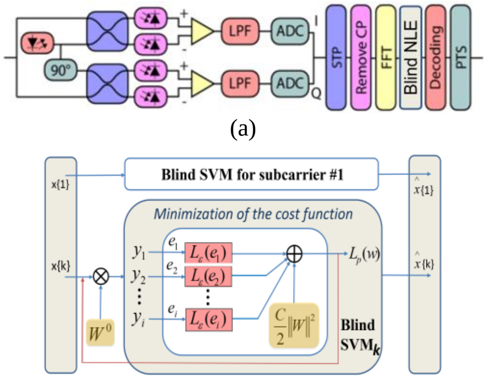

(a)

(b)

Fig. 2. (a) Block diagram of CO-OFDM receiver with BNLE. (b) Proposed SVM-BNLE.

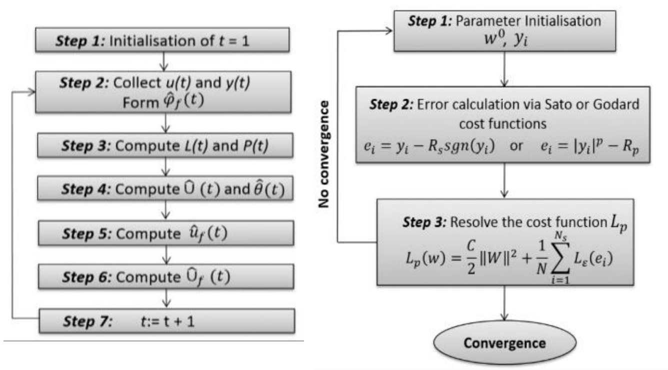

(a) (b)

Fig. 3. (a) Flowchart for computing the ML-RLS estimate $\hat{\theta}(t)$. (b) IRWLS pseudocode.

II. Proposed Algorithm

The proposed approach extracts high-order statistics indirectly from error functions defined over the NLE output leading to stochastic gradient descent algorithms. The proposed BNLE employs the Sato's [9] and Godard's-based constant modulus algorithm (CMA) [9] cost functions in the penalty term of an SVM-like cost function which is iteratively minimized by IRWLS. Fig. 1 depicts (a) the block diagram of the CO-OFDM receiver equipped with the BNLE, and (b) the proposed SVM-BNLE. The received OFDM symbols for each subcarrier $x\{k\}$ are processed by BNLE which are scaled by the vector of filter coefficients (weights, w) for each subcarrier $w_{k,i}$ (where i is the symbol) by means of ML-RLS [10]. Assume we have a set of N_s number of subcarriers with u, the system input and y, the output: $u_N=\{u(1),u(2),\ldots,u(N_s)\}$, $y_N:=\{y(1),y(2),\ldots,y(N_s)\}$. Let the likelihood function $L(y_{Ns}|u_{Ns-1},\theta)$ equal the probability density function $p(y_{Ns}|u_{Ns-1},\theta)$. The ML estimate is then obtained by maximizing the likelihood, i.e. $\hat{\theta}_{ML} = \underset{\theta}{\operatorname{argmax}}\, L(y_{Ns}|u_{Ns-1},\theta)$. Assuming an ML-RLS system which employs a nonlinear FIR and the ML estimates $\hat{\theta}_{ML} = \hat{\theta}(t-1)$, the Taylor expansion of $U(t)$ can therefore be expressed as $\hat{\theta}(t) = \hat{\theta}(t-1) + L(t)\hat{U}(t)$, in which the $L(t)$ term is derived from $L(t) = P(t-1)\hat{\varphi}_f(t)/[1+\hat{\varphi}_f^T(t)P(t-1)\,\hat{\varphi}_f(t)$; where $\hat{\varphi}_f(t)$ is the information vector [10] and $P(t-1)$ is the covariance matrix.

The flowchart for computing the ML-RLS for blind nonlinear operation that estimates $\hat{\theta}(t)$ (=$\hat{\theta}_{ML}$) is shown in Fig. 3(a). Hence, using ML-RLS the BNLE output in a more general form becomes:

$$y_k = \sum_{n=0}^{N_s-1} w_{k,i}x_{k-n} = x_k^T w_{k,i} \tag{1}$$

In (1) we assume a reference sequence s_k to obtain the optimal coefficients for linear operation. Hereafter, the equalizer updates the weights, w, in (1) with the help of the following expression [10]:

$$w_{k+1} = w_k + \eta e_k x_k^H, \tag{2}$$

where H denotes the Hermitian operator, η the step-size, and e_k the error of the equalizer output, $e_k = y_k - s_{k-d}$, with d being the joint channel-equalizer delay. Formulation of the proposed equalizer is performed by means of the IRWLS algorithm to solve a cost function obtained from the SVM framework. For a subcarrier number, N_s, the proposed algorithm minimizes the following SVM-based cost function:

$$L_p(w) = \frac{C}{2}\|W\|^2 + \frac{1}{N_s}\sum_{i=1}^{N_s} L_\varepsilon(e_i), \tag{3}$$

where $L_\varepsilon(e_i)$ is the loss function, C is a penalty regulation parameter (indicated as C-parameter in Fig. 5(b)), and e_i is the penalization term for the i^{th} symbol. The loss function denotes the existence of an ε-insensitive region of size ε by means of quadratic cost function:

$$L_\varepsilon(e) = \begin{cases} 0\,,\ if\ e < \varepsilon \\ e^2 - 2e\varepsilon + \varepsilon^2, if\ e \geq \varepsilon \end{cases} \tag{4}$$

In this context, the BNLE consists in replacing the reference signal in the error term e_i by Sato and Godard reference, i.e.

— *Sato cost function*:

$$e_i = y_i - R_s sgn(y_i), \tag{5}$$

where $R_s sgn(y_i)$ is a statistical reference and R_s is Sato's constant.

— *Godard cost function*:

$$e_i = |y_i|^p - R_p, \tag{6}$$

where R_p is the Godard's constant. From (6) we consider $p = 2$, which is the most common choice for Godard algorithms (this is the order that defines the CMA on-line algorithm). The steps involved (initialize W^0) in SVM-BNLE using the IRWLS pseudocode are shown in Fig. 3(b), in which $L_\varepsilon(e)$ is calculated from (5) and (6) via (1) by substituting $y_i = y_k$.

The adopted VNLE procedure is identical to Ref. [7] using 3rd order Volterra Kernels, thus offering ~50% reduced computational DSP complexity compared to single-step/span DBP. Such VNLE inherits some of the features of the hybrid time-and-frequency domain implementation, for instance non-frequency aliasing and simple implementation using parallel processing for concurrent CD and fiber nonlinearity compensation.

III. Experimental Setup and Results

Fig. 4 depicts the experimental setup for (a) single- and (b) multi-channel CO-OFDM where external cavity lasers of 100 KHz linewidth were modulated using a dual-parallel Mach-Zehnder modulator fed with ‘offline’ OFDM IQ components. The transmission path at 1550.2 nm was a recirculating loop consisting of 20×100 km (single-channel; 4-spans × 100km × 5 rounds) and 32×100 km spans (multi-channel; 4-spans × 100 km × 8 rounds) of OH-LITE fiber (attenuation of 18.9-19.5 dB/100 km) being switched by an acousto-optic modulator. The loop switch was located before the 1st Erbium-doped fiber amplifier (EDFA) and a gain-flattening filter was placed after the 3rd EDFA for both configurations to flatten the gain across the wavelengths of interest. For Fig. 4(b), the transmitter was constituted of five distributed feedback lasers on 100 GHz grid located between 193.5–193.9 THz connected with a polarization maintaining multiplexer. Using an amplified spontaneous emission (ASE) source, another 20 ‘dummy’ channels of 10 GHz bandwidth were generated with a channel spacing of ~ 100 GHz. These channels covered 2.5 THz of bandwidth as depicted in inset Fig. 5(b). The optimum launched optical power (LOP) was swept by controlling the output power of the EDFAs. At the receiver, the incoming signal was combined with 100 KHz linewidth local oscillator for both single- and multi-channel configuration.

After down-conversion, the signal was sampled using a real-time oscilloscope operating at 80 GS/s and processed offline in *Matlab*. 400 OFDM symbols were generated using a 512-point IFFT, 210 middle subcarriers were modulated using 16-QAM while the rest were set to zero. A cyclic prefix of 2 % was included to eliminate ISI. The OFDM demodulator for non-blind LE/VNLE included timing synchronization, IQ imbalance, CD and frequency offset compensation [7] resulting in a net bit-rate of ~20 and ~40-Gb/s for QPSK and 16-QAM CO-OFDM, respectively. All NLEs were assessed by Q-factor measurements (related to bit-error-rate, BER, using $Q = 20log_{10}[\sqrt{2}erfc^{-1}(2BER)]$) averaging over 10 recorded traces (~10^6 bits), which was estimated from the BER obtained by error counting after hard-decision decoding.

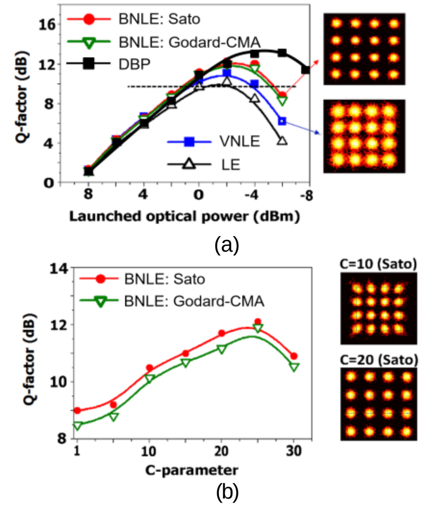

Fig. 5. (a) Q-factor vs. launched optical power (LOP) at 2000 km for single-channel 16-QAM CO-OFDM using BNLEs (~41-Gb/s) and VNLE/LE/DBP (40-steps/span) (~40-Gb/s). (b) Q-factor vs. *C*-parameter for BNLEs at optimum LOP of 2 dBm. Insets: Received constellation diagrams at (a) 6 dBm of LOP for Sato-BNLE and VNLE; and (b) for Sato-BNLE with a C-parameter of 10 and 20.

In Fig. 5 (a), the Q-factor against the LOP is plotted for single-channel CO-OFDM at 2000 km for BNLEs at ~41-Gb/s, and for non-blind LE, VNLE, and DBP at ~40-Gb/s. It is shown that for an optimum LOP of 2 dBm, BNLEs can reduce the fiber nonlinearity penalty by ~1 and ~2 dB compared to VNLE and LE, respectively. The performance benefit of the BNLE is also clear for high powers, as depicted in the received constellation diagrams at 6 dBm of LOP shown as inset in Fig. 5(a) (upper diagram: BNLE-Sato; lower diagram: VNLE). BNLEs can also extend the range of LOP by up to ~3.5 dB at the FEC-limit (~10 dB in Q-factor). However, when compared to DBP the Q-factor is lower for high LOPs. On the other hand, Sato slightly enhances the Q-factor compared to Godard-CMA, due to the ability of tackling stochastic nonlinear phase variations. Fig. 5(b) confirms such improvement in terms of the *C*-parameter, where by proper *C*-parameter scaling the BNLE performance can be enhanced by ~3.5 dB.

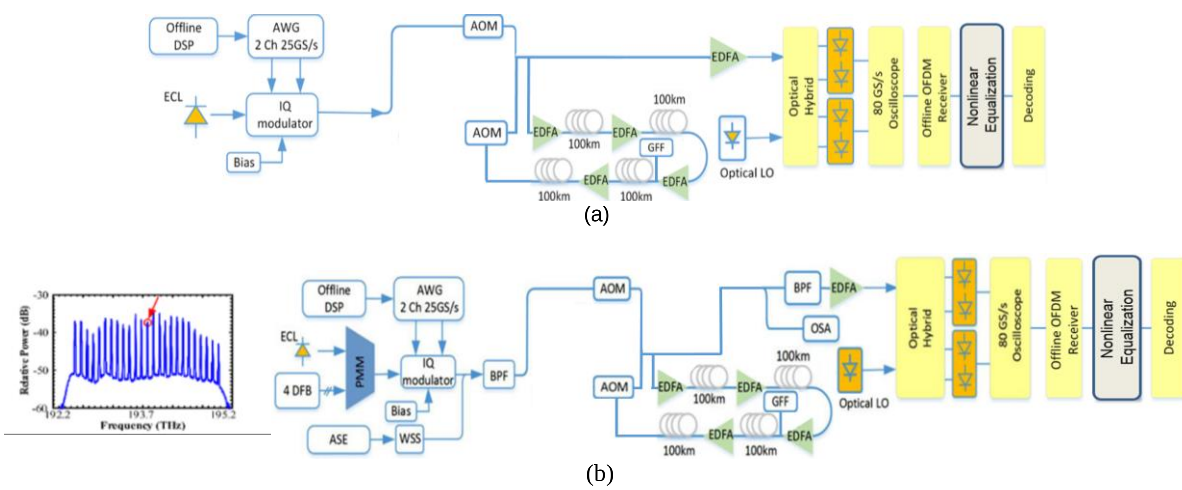

Fig. 4. Experimental setup for (a) single- (b) multi-channel configuration. Inset: Received spectrum for multi-channel system. DSP: digital signal processing, ECL: external cavity laser, AWG: arbitrary waveform generator, AOM: acousto-optic modulator, EDFA: Erbium-doped fiber amplifier, GFF: gain-flattening filter, LO: local oscillator, DFB: distributed feedback laser, ASE: amplified spontaneous emission, PMM: polarization maintaining multiplexer, WSS: wavelength selective switch, BPF: bandpass filter, OSA: optical spectrum analyzer.

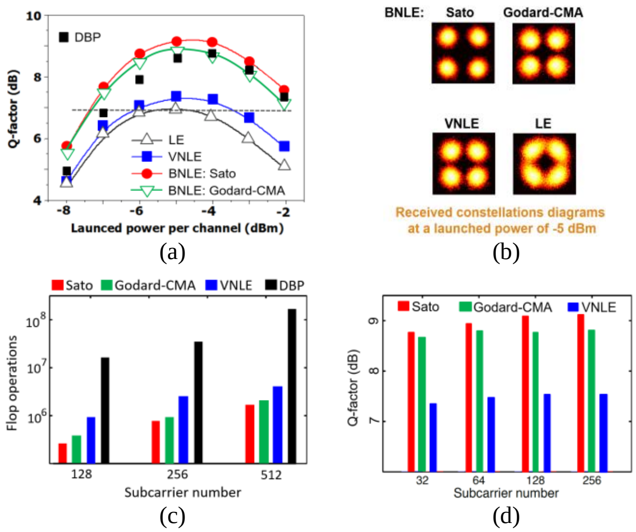

Fig. 6. (a) Q-factor vs. LOP at 3200 km for middle-channel QPSK multi-channel CO-OFDM using BNLEs (~21-Gb/s) and VNLE/LE (~20-Gb/s). (b) Received constellation diagrams for NLEs at optimum LOP of -5 dBm. (c) Complexity comparison of algorithms at 2000 km. (d) Q-factor vs. subcarriers at 3200 km and optimum LOP (-5 dBm) for a simulated QPSK multi-channel CO-OFDM.

In Fig. 6(a), the Q-factor against the LOP is plotted for multi-channel QPSK CO-OFDM at 3200 km for BNLEs at ~21-Gb/s, and for LE/VNLE/DBP at ~20-Gb/s. As shown from the results in Fig. 6(a) and the corresponding received constellation diagrams at optimum -5 dBm of LOP in Fig. 6(b), an improvement in Q-factor of ~1.7 dB is observed using Sato-BNLE compared to VNLE. On the other hand, results reveal that Sato slightly outperforms Godard-CMA for optimum and high LOPs. Moreover, the proposed BNLE is very effective for multi-channel CO-OFDM as it outperforms the 'gold-standard' DBP over the whole range of LOPs (BNLE can tackle the stochastic parametric noise amplification). Our results show that the proposed BNLE can tackle more effectively inter-channel nonlinear cross-talk effects than intra-channel nonlinearities. It should be noted that at low powers the proposed BNLE can improve the Q-factor compared to LE/VNLE since it partially tackles the interaction of the accumulated stochastic ASE noise with other effects at 3200 km (many optical amplifiers involved). Finally, in Fig. 6(d) we numerically investigate in a co-simulated Matlab® (electrical/DSP components) with VPI™-transmission-maker (optical devices and standard single-mode fiber) platform the impact of the number of subcarriers on BNLEs in ~21-Gb/s QPSK multi/middle-channel CO-OFDM at 3200 km and optimum LOP of -5 dBm. From Fig. 6(d), it is evident that for higher number of subcarriers Sato-BNLE is more robust than Godard-CMA and VNLE, because it can tackle more effectively the accumulated inter-subcarrier FWM induced from CO-OFDM's high PAPR [6,7]. The numbers of floating-point real-valued operations (FLOP) for VNLE is calculated by $N_{VNLE} = (N_{span} + 1)8N_{SC}Klog_2(N_{SC}K) + (20N_{span} - 6)N_{SC}K + 16(N_{span} + 1)$, and for DBP by $N_{DBP} = d_{link}/d_{step}[8N_{SC}Klog_2(N_{SC}K) - 9KN_{SC} + 16]$, where N_{span} is the span number, K the oversampling factor, N_{SC} the subcarrier number, d_{link} the distance and d_{step} the splitting step. The BNLE FLOP is independent from the link-related parameters and is calculated by $N_{Godard} = N_{SC}KN_i[12N_w + \left(\frac{64}{3}\right)N_s^3 + (3p + 20)N_s^2 + (p + 2)N_s + 2]$ and $N_{Sato} = N_{SC}KN_i[12N_w + \left(\frac{64}{3}\right)N_s^3 + 21N_s^2 + 3N_s + 2]$, where N_i, N_w, N_s are the number of iteration, the filter order and training data, respectively. p=2 for the CMA and N_s is 1 since our algorithm is blind. For a system with $N_{SC} = 512, K = 4, N_{span} = 20, d_{link} = 2000$ km, d_{step} = 2.5 km, $N_i = 10$ (related to C-parameter) and N_w=3, the BNLE is minimum about 70.7 and 2.5 times less complex than DBP and VNLE, respectively. Fig. 6(c) shows a FLOP comparison between the BNLEs and VNLE/DBP for different N_{SC} at 2000 km.

IV. Conclusion

A novel ML-RLS-based SVM-BNLE was experimentally demonstrated harnessing Sato and Godard-CMA for single-channel 16-QAM CO-OFDM and multi-channel QPSK CO-OFDM over up to 3200 km of fiber transmission. Compared to VNLE, BNLE reduced the fiber nonlinearity penalty especially when considering inter-channel nonlinearities (~1.7 dB in Q-factor at optimum transmitted power of -5 dBm) and high number of subcarriers. Sato marginally outperformed Godard-CMA by tackling more effectively stochastic nonlinear phase variations. Compared to DBP, BNLE outperformed for multi-channel QPSK since DBP cannot tackle inter-channel nonlinear cross-talk effects.

References

[1] R. Maher et al., "Spectrally shaped DP-16QAM super-channel transmission with multi-channel digital back-propagation," *Nature Scient. Rep.*, vol. 5, 8214, 2014.

[2] Y. Yu and J. Zhao, "Modified phase-conjugate twin wave schemes for fiber nonlinearity mitigation," *Opt. Exp.*, vol. 23, no. 23 pp. 30499–30413, 2015.

[3] M. Khairuzzaman et al., "Equalization of nonlinear transmission impairments by maximum-likelihood-sequence estimation in digital coherent receivers," *Opt. Exp.*, vol. 18, no. 5, p. 4776–4782, 2010.

[4] T. Nguyen et al., "Fiber nonlinearity equalizer based on support vector classification for coherent optical OFDM," *IEEE Phot. J.*, vol. 8, no. 2, 2016.

[5] S. Mhatli, H. Mrabet, I. Dayoub, and E. Giacoumidis, "A novel SVM robust model Based Electrical Equalizer for CO-OFDM Systems," *IET Commun.*, vol. 11, no. 7, pp. 1091–1096, 2017.

[6] E. Giacoumidis et al., "Comparison of DSP-based nonlinear equalizers for intra-channel nonlinearity compensation in coherent optical OFDM," *Opt. Lett.*, vol. 41, no. 11, pp. 2509–2512, 2016.

[7] E. Giacoumidis et al., "Experimental Comparison of Artificial Neural Network and Volterra based Nonlinear Equalization for CO-OFDM," in Proc. OFC, W3A.4, Anaheim (2016).

[8] S. T. Le et al., "Decision-Directed-Free Blind Phase Noise Estimation for CO-OFDM," in Proc. OFC, W1E.5, Anaheim (2015).

[9] M. Lázaro et al., "Blind equalization using the IRWLS formulation of the support vector machine," *Signal Proc.*, vol. 89, no. 7, p. 1436–1445, 2009.

[10] J. Li et al., "Maximum likelihood least squares identification method for input nonlinear finite impulse response moving average systems," *Math. & Comp. Model.*, vol. 55, p. 442–450, 2012.

[11] F. Chen and F. Ding, "The filtering based maximum likelihood recursive least squares estimation for multiple-input single-output systems," *Appl. Math. Model.*, vol. 40, no. 3, p. 2106–2118, 2016.